



## Paleoseismology of the Itoigawa-Shizuoka tectonic line in central Japan

Koji Okumura

*Department of Geography, Graduate School of Letters, Hiroshima University Higashi-Hiroshima, 739-8522 Hiroshima, Japan; e-mail: kojiok@hiroshima-u.ac.jp*

Received 12 July 1999; accepted in revised form 10 October 2000

*Key words:* paleoseismology, reverse-fault, risk assessment, slip-rate, strike-slip fault, trenching

### Abstract

The 150-km-long Itoigawa-Shizuoka tectonic line active fault system (ISTL) in central Japan is one of the most active Quaternary fault systems in Japan. Estimated slip-rates on the fault system are as large as 10 m/ka, but the historic seismicity has been low since 841 A.D. with no large earthquakes recorded. The high slip rates contrast with the long time since the last major earthquake on the ITSL and indicates the high potential of a large earthquake from the ISTL. Based on slip-rate estimates, more than 10 m of potential slip may have accumulated on the fault system since the 841 A.D. earthquake. Recent paleoseismological studies on the middle and northern parts of the ISTL have determined that the average recurrence interval of surface-faulting earthquakes on the middle ISTL is 680 to 825 years (Gofukuji fault) and 1258 to 1510 years in the northern ISTL. These data suggest the most recent event on both northern and middle ISTL occurred in 841 A.D. The results highlight the high seismic potential of the ISTL. Additional studies of the entire ISTL are needed to define the extent of the next rupture.

### Introduction

The Itoigawa-Shizuoka tectonic line is a major Miocene-Pliocene fault system that separates south-western from northeastern Japan, and may be the present-day plate boundary between the Okhotsk (or North American) and Amurian (or Eurasian) plates (Figure 1: Seno and Sakurai, 1996; Wei and Seno, 1998). During the Miocene, an extensive sedimentary basin developed in a half graben on the east side of the fault system. The fault system was probably an east-dipping normal fault system that developed in an E-W extensional stress field (Sato, 1996). East of the tectonic line, the north-south-trending, 100- to 200-km-wide sedimentary basin, named the Fossa Magna cut across central Japan and continued to subside until Early to Middle Pliocene.

In early Pleistocene, the central portion of the tectonic line was reactivated under E-W compressional stress, and developed into the Itoigawa-Shizuoka tectonic line active fault system (abbreviated as ISTL in this paper: Figure 1). The ISTL is one of the fastest-moving onshore fault systems in Japan. Estimates of

the average slip rate in late Quaternary are between 5 to 14 m/ka (Ikeda and Yonekura, 1986; Fujimori, 1991; Okumura et al., 1994).

The system can be divided into three distinct segments; the Northern, the Middle, and the Southern ISTL. The Northern ISTL consists east-dipping reverse faults extending 60 km. The Middle ISTL is a 50-km-long zone of NW-SE trending cluster of left-lateral strike-slip faults from Matsumoto to Kobuchizawa, and the Southern ISTL consists of west-dipping reverse and thrust faults extending about 50 km from Kobuchizawa to Kajikazawa (Figure 1).

The spectacular fault topography and the geomorphic evidence of high activity on the ISTL has long been recognized (e.g. Allen, 1975). Although many studies have been carried out in this region (See: Research Group for Active Faults in Japan, 1991), the researchers did not recognize the potential for a large earthquake on the ISTL in the near future until the 1990s. The conclusion from several paleoseismological trench sites in 1980s indicated that the last event had occurred in 841 A.D. and the average recurrence interval was 3500 to 5000 years (Research Group for

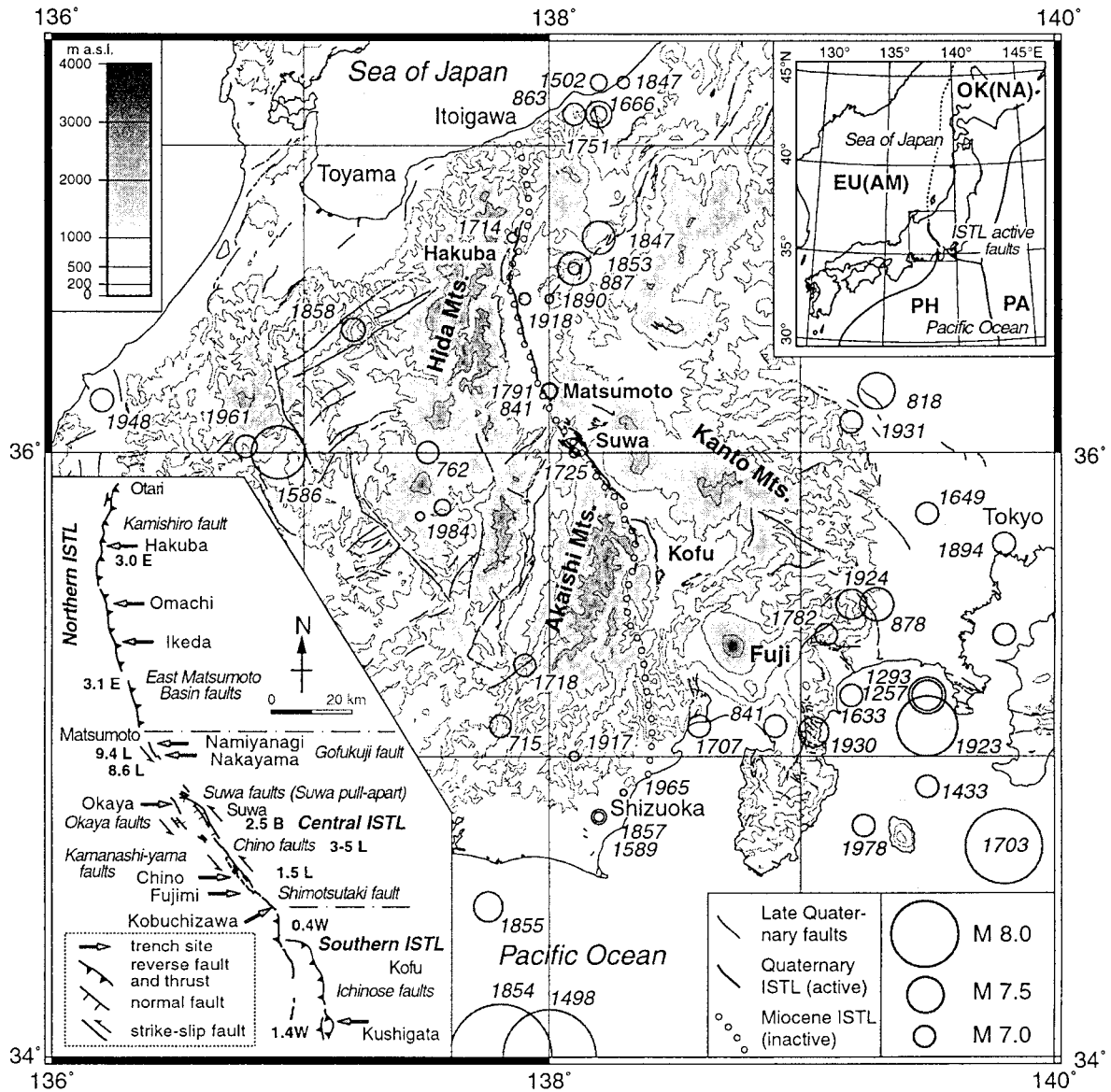


Figure 1. Late Quaternary faults and large historic earthquakes in and around central Japan. Late Quaternary faults: Research Group for Active Faults in Japan (1991) and Working Group for Compilation of 1:2,000,000 Active Fault Map of Japan (2000), Epicenters: Utsu (1996), Topographic map: 1 km DEM of Geographical Survey Institute (1997) mapped using GMT (Wessel and Smith, 1995). Plate division and boundaries (inset upper right) are based on Seno and Sakurai (1996) and Wei and Seno (1998). EU: Eurasian, AM: Amurian, OK: Okhotsk, NA: North American, PH: Philippine Sea, and PA: Pacific Plates. Outline of the Itoigawa-Shizuoka tectonic line [ISTL] active fault system and sites of exploratory trenches (inset lower left) are based on Shimokawa et al. (1995). Numbers indicate average slip rate of the faults in m/ka E: east-side-up vertical component, W: west-side-up vertical component, L: left-lateral, and B: subsidence of Suwa pull-apart basin.

Ito-Shizu Tectonic Line Active Faults, 1988; Togo et al., 1988). However, the discrepancy between an apparent long recurrence interval and high slip rate was not further investigated.

Recently, Okumura et al. (1994) reported that the recurrence interval was less than 1000 years along the Middle ISTL, and subsequent research by Okumura et al. (1998b) demonstrated that the recurrence interval along the Northern ISTL was 1000–1800 years. In both areas, the last event was supposed to have occurred either in A.D. 762 (Matsuda, 1998) or in A.D. 841 (Usami, 1996) based on historic records. This information led the Earthquake Research Committee of the Government of Japan to issue an official warning in September 1996 regarding the risk of a large earthquake along the ISTL (Headquarters for Earthquake Research Promotion, 1996). The warning is an important step for the long-term effort for the earthquake hazard mitigation in Japan after the disaster of the 1995 Hyogo-ken Nanbu (Kobe) earthquake. This paper summarizes the results of the paleoseismological investigation along ISTL that contributed to the first long-term earthquake hazard assessment in Japan, together with the most recent results from ongoing studies.

### **Paleoseismology of the Gofukuji Fault, Middle ISTL**

#### *High slip-rate and low seismicity*

The Middle ISTL is characterized by high average slip-rate reaching 5 to 14 m/ka during the Late Pleistocene and Holocene (Ikeda and Yonekura, 1986; Okumura et al., 1994; Fujimori, 1991). This is one of the highest slip-rates reported for onshore active faults in Japan. Since the largest slip-per-event ever observed in Japan is 9 m (during 1891 Neodani earthquake: Matsuda, 1974), this slip-rate indicates that the recurrence time along the Middle ISTL must be about 2000 years or much shorter. The previously reported recurrence time estimates of 3500 to 5000 years from ISTL (Figure 13: Okaya and Chino: Research Group for Ito-Shizu Tectonic Line Active Faults, 1988; Togo et al., 1988) were significantly longer than the recurrence time inferred from the slip rate. The last surface-rupturing earthquake on the Middle ISTL must have occurred in 762 A.D. or 841 A.D. according to historical records and paleoseismological research (Usami, 1996; Matsuda, 1998). Because the elapsed time since

the last surface-rupturing earthquake is 1159 or 1238 years, the estimate of recurrence time is critical to evaluate the potential of the next earthquake. In the discussion hereafter, the author will only cite the A.D. 841 earthquake for simplicity. The significance of the possible A.D. 762 earthquake will be discussed in section 4.

To determine the history of recent faulting events, three trenching studies were carried out on the Gofukuji fault, the northernmost segment of the Middle ISTL at Namiyanagi (in 1988 and 1990) and Nakayama (in 1996), south of Matsumoto (Figure 2). These studies involved investigations of 6 trenches, three test pits and topographic mapping of the areas around the trenches. Interpretation of the mapping and dating of paleo-earthquakes yielded the following results. Most data from the Namiyanagi trenches were published by Okumura et al. (1994 and 1998b) in Japanese. This chapter re-examines these results together with new findings from the Nakayama trenches to present the updated paleoseismological information on the Middle ISTL.

#### *Outline of the Gofukuji fault*

A series of distinctive pressure ridges along the Gofukuji fault provide evidence of recent high activity of the fault in southeastern corner of the Matsumoto Basin (Figure 2A, Figure 6 inset). Along its NNW-SSE linear trace, the fault produces several left-laterally offset streams and terrace risers, and forms both east-facing and west-facing fault scarps that offset Late Pleistocene to Holocene alluvial-fan and terrace surfaces. The clear topographic expression of the Gofukuji fault extends only 8 km. The fault's possible northern continuation extends from Namiyanagi and passes the downtown of Matsumoto city under modern alluvial-fan surface for 3 to 4 km (Figure 2). And the 10-km southernmost portion of the EMBF (East Matsumoto Basin fault) under the present riverbed could belong to the Gofukuji fault.

To the south between the Gofukuji fault and the Okaya fault (left-lateral strike-slip: Figure 1), there is a 9-km-long gap in over 2000-m-high mountains. The origin of this gap is not certain yet. One possibility is that a through-going fault exists in this area, but erosion is so severe that even the most recent evidence of faulting is erased. Another possibility is that the mountainous area is within a compressional left stepover that has caused uplift of the mountains at a

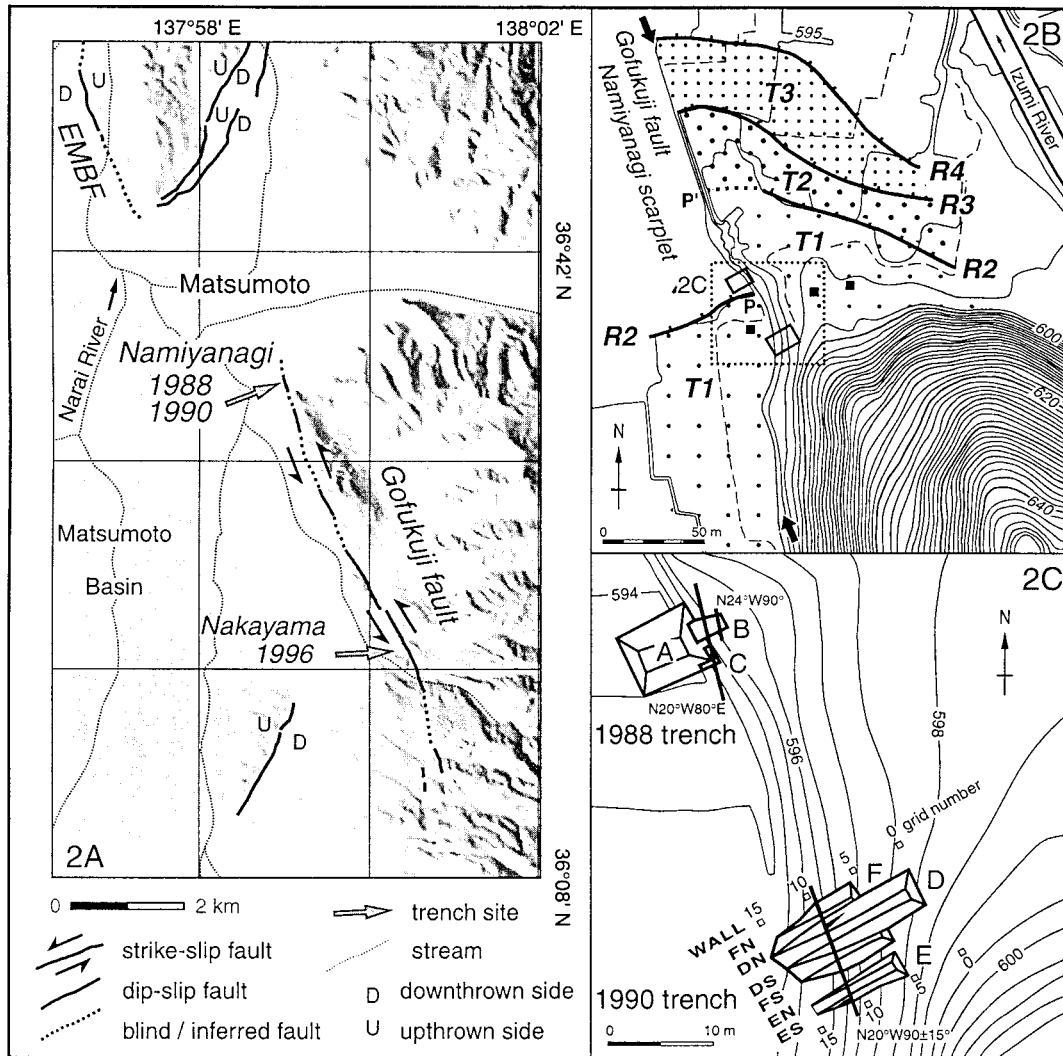


Figure 2. 2A (left): Topography around the Gofukuji fault based on 50 m DEM of Geographical Survey Institute (1997) mapped using GMT (Wessel and Smith, 1995). 2B (upper right): Map of offset terraces around the Namiyanagi trench site. P and P' indicate the piercing points of the terrace riser R2. Solid squares are test pits. Detailed topographic map is unpublished data of the Topography Section, Geological Survey of Japan. 2C (lower right): Plan view of the Namiyanagi trenches. Each wall is named after trench name (A, B, C, D, E, F) plus North (N) or South (S). Detailed topographic map is unpublished data of the Topography Section, Geological Survey of Japan. Small black patch on DN and ES walls are unit s2a, which indicates the slip by the last event (modified from Okumura et al., 1994, Figures 3 and 4).

restraining bend. Though the Gofukuji fault's length is very uncertain, its maximum length is 20 to 30 km.

#### *Namiyanagi trench site: Fault topography and slip-rate estimates*

The 1988 and 1990 trenches at Namiyanagi were dug into a sharp west-facing fault scarplet that offsets a series of Holocene fluvial terrace surfaces formed by the Izumi River (Figure 2B). Although the topography

around the scarplet is extensively modified by human activities, the terrace risers provide piercing points to estimate the rate of left-lateral strike-slip. Among the three terrace risers in east side, the R2 riser is correlated with the R2 riser in west side. The correlation is based on the stratigraphy and the radiocarbon dates of the T1 terrace deposits in the 1988 A trench and three test pits. The offset of the piercing points PP' is about 60 m (Figure 2). Considering the uncertainty of the exact location of P' due to human modification, the offset

is estimated to be between 40 to 80 m. This amount of offset combined with the radiocarbon age of the R2 riser between 8200 and 5800 Cal. y. B.P. indicates an estimated left-lateral slip-rate of 5–14 m/ka (Okumura et al., 1994). This estimate coincides with that of Ikeda and Yonekura (1986) at Nakayama ( $8.6 \pm 1.0$  m/ka during 55 ka). The west-side-down vertical component of the slip rate is around 0.6 m/ka, and is less than one-tenth of the strike-slip component. This vertical component might be related to the left stepover of the fault system across Matsumoto city (Figure 2).

#### *Namiyanagi trenches*

The Namiyanagi 1988 excavation consisted of a main trench (A) and two sub-trenches (B and C in Figure 2C). The fault plane was not exposed at the foot of the scarp in the A trench. In the B trench, two subvertical fault strands are visible, but the fault planes were truncated by recent, probably artificial fill. In this trench, there was no deposit and structure that allows an estimate of the age of the most recent events. Only two older events that occurred around 2881 to 3316 Cal. y. B.P. (age of a wood sample from the horizon at an upper termination of a subsidiary fault in A trench) and around 8000 Cal. y. B.P. were dated (Okumura and Tsukuda, 1995). The radiocarbon dates reported hereafter are dendro-corrected age in  $1\sigma$  range, calibrated using CalibETH1.5b (Niklaus, 1991). Though it was not possible in 1988 to estimate the recurrence intervals and the elapsed time since the last event, repeated events in these 3000 years were evident from the stratigraphic relations and structures in the trenches.

Following the indication of high activity in 1988 trenches, additional trenches were excavated at Namiyanagi in 1990. Clear evidence of the three latest earthquake events in the past 3000 years was exposed in these trenches. Two trenches (D and E; Figure 2C) were opened about 30 m south of the A trench. After initial examination of trench D, we widened the western half of this trench. Trench F is composed of a pair of retreated walls as shown in the plan view in Figure 2C. The master fault zone, which is a negative flower structure, consists of F1, F2, and F3 fault planes, and juxtaposes terrace deposits on the east with marsh deposits on the west at around the 10 m grid line (Figures 3, 4, and 5).

The fluvial gravel and sand on the east side (units e1, e2, and e3) compose the T1 terrace surface that has an age of 8200 to 7800 Cal. y. B.P. These terrace deposits overlie Late Pleistocene sand and silt

layers (P), which are sliced and overturned by subsidiary faults. The marsh deposits on the west side (unit w1) consist of humic sand and silt that contains 2000 to 2500 y. B.P. pottery fragments (personal communication: Matsumoto City Board of Education) near the top. The archaeological age of the pottery agrees with radiocarbon ages (DN-9 in Figure 4 and ES-3 in Figure 5). Overlying these terrace and marsh deposits, slope deposits (s1 and s2) are mixtures of reworked terrace gravel and sand mixed with humic A-horizon material. There is large diversity in the organic content of the slope deposits, but their sedimentary structures indicate their colluvial origin.

Each unit of the slope deposits in the trench walls has a characteristic lithology, texture, sedimentary sequence, and age. Among these slope-deposit units, unit s2a on the east side of fault F2 on the DN wall (Figure 4) has identical features and dates as unit s2a on the west side of fault F2 on the ES wall (Figure 5). Thus, the same units are found only on DN and ES walls. Hence, it is very likely that before the rupture of F2 fault, a lobe of slope deposits (unit s2a) was lying on the fault zone, and during the faulting event, this lobe was left laterally offset by the faulting. Based on the estimated width of the lobe along the fault and present separation, the slip on fault F2 is 6–9 m since the deposition of unit s2a. This is the amount of slip that was associated with the last faulting event, and is the only estimate of the slip-per-event on the Gofukuji fault.

#### *Recognition of faulting events and their ages in Namiyanagi trenches*

Four faulting events, named event Z, Y, X, W in ascending order, are recognized and dated in Namiyanagi trenches.

Event Z, the last event from the Gofukuji fault, is recognized by stratigraphic relations between units s1 and s2 on all trench walls. The fault plane F2 cuts all units below unit s1, unit s1 obviously truncates fault F2, and unit s1 lies undeformed on the scarp slope. This upper termination of the fault planes is common in all of the trenches (Figures 3, 4, and 5), and thus this is strong evidence of the last event. This event predates the radiocarbon dates of ES-4, DN-7, DN-11, and DS-18, and postdates those of ES-5 and DS-9. The preferred age of the event Z is older than sample DN-7 (bulk humic soil,  $\beta$ -counting: 723–564 Cal. y. B.P.) and younger than sample ES-5 (bulk humic soil,  $\beta$ -counting: 1505–1348 Cal. y. B.P.). Because sample

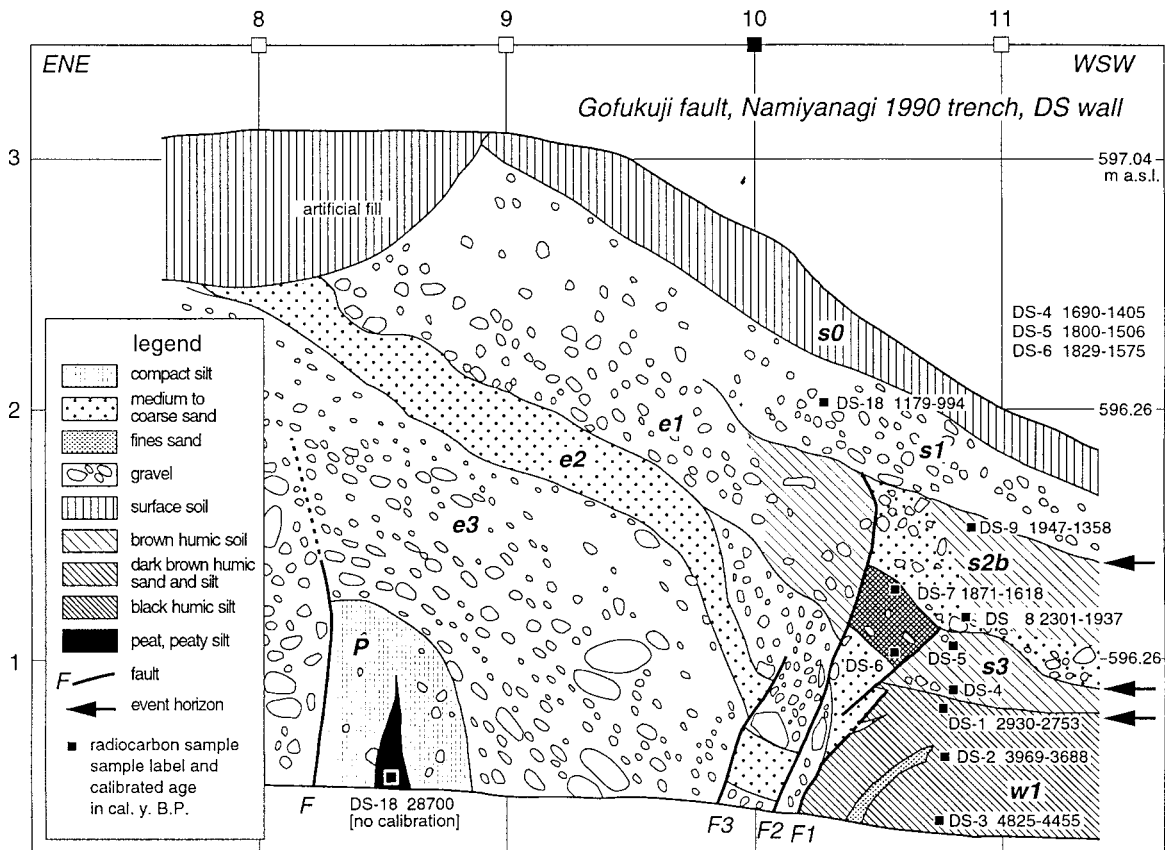


Figure 3. Map of the fault zone on the DS wall (modified from Okumura et al. 1994, Figure 6). The ordinate is actual length on slant wall of 50 to 60°.

DN-7 is from a horizon that is the least disturbed by soil creep on the slope and minimizing contamination by mixing of organic material, and sample ES-5 yielded the youngest date for unit s2a from an apparently uneroded top of the unit. Thus event Z occurred between about 1500 and 500 Cal. y. B.P.

The evidence of Event Y is indicated by another distinctive upper termination of fault planes just below unit s2 (Figures 3 and 5). Fault plane F1 cuts all units of s3 and below, and unit s2 truncates fault F1. Event Y predates the radiocarbon samples of ES-6 and DS-8, and postdates samples DN-10, DS-4, and DS-5. The samples from within the fault zone (DS-6, DS-7, ES-7) are not used to bracket the age of this event because of the severe disturbance affecting these deposits. The preferable age of the event Y is older than sample ES-6 (bulk humic soil,  $\beta$ -counting: 1823–1616 Cal. y.

B.P.) and younger than sample DS-5 (bulk humic sand,  $\beta$ -counting: 1800–1506 Cal. y. B.P.). Sample ES-6 was collected from the lowest part of unit s2a and is expected to have the least contamination after deposition. The contact between units s2a/b and s3 is usually unconformable, and erosion is inferred. Sample ES-6 was deposited shortly after the event and its date represents a minimum age for event Y. Following event Y, fault F1 was buried by unit s2a/b.

Event X is recognized from the internal deformation in unit w1 adjacent to fault F1. A thin sand layer in unit w1 on the DS wall dips steeply toward fault F1, indicating drag deformation associated with faulting (Figure 3). A black, humic, silt layer in the upper part of unit w1 on the DN wall is also strongly deformed adjacent to the F1 fault plane (Figure 4). This deformation within unit w1 unit does not affect unit s3 or

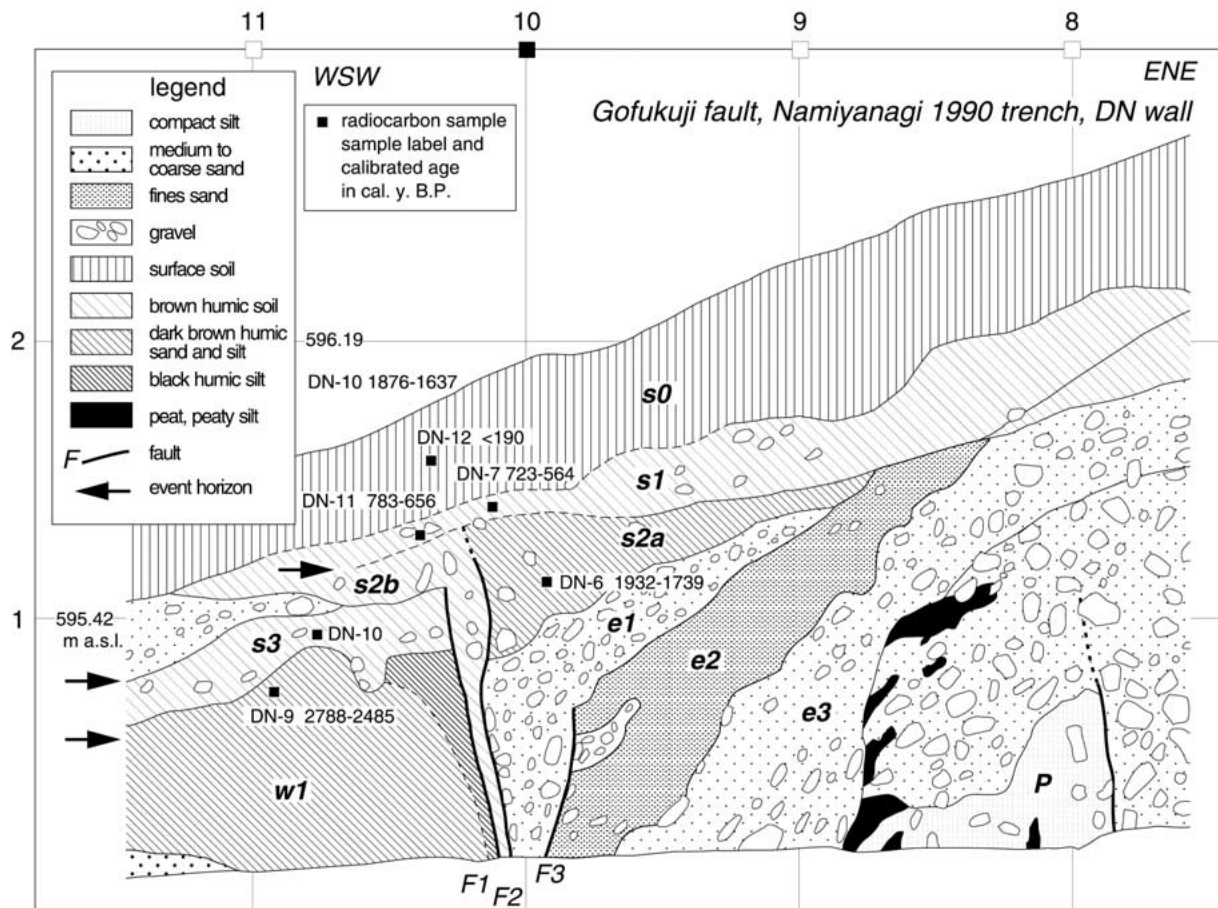


Figure 4. Map of the fault zone on the DN wall (modified from Okumura et al. 1994, Figure 7). The ordinate is actual length on slant wall of 50 to 60°.

shallower deposits. Unit w1 is unconformably covered by the unit s3, therefore, the deformation of the uppermost part of unit w1 took place before the deposition of unit s3. The mode of this plastic deformation is different from the brittle faulting during Y and Z events, however, this deformation was associated with slip on the Gofukuji fault.

Thus, the event X is occurred during deposition of the uppermost part of unit w1 or in the time interval between deposition of unit w1 and unit s3. The former timing is more probable because unit s3 does not contain any pieces of unit w1, which indicates that deposition of unit s3 did not immediately follow the deformation and erosion of unit w1. The age of the event X predates the deposition of sample ES-8 (bulk humic sand in uppermost unit w1,  $\beta$ -counting: 2335–2138 Cal. y. B.P.) and postdates sample DN-9 (bulk humic sand below the deformed black silt,  $\beta$ -

counting: 2788–2485 Cal. y. B.P.). Event W is one of the oldest events recognized in the 1988 A trench and is dated as 2881 to 3316 Cal. y. B.P. (see section 2–4). Though there are no other events recognized between the events X and W, structural evidence in the Namiyanagi trenches does not demonstrate that event W was directly followed by the three successive events identified in 1990 trenches. The timing and order of event W will be discussed later together with the results from the Nakayama trenches.

The three most recent faulting events on the Gofukuji fault occurred, in 564 to 1505, 1800 to 1616, and 2788 to 2138 Cal. y. B.P. Assuming the timing of the last event to be 1109 Cal. y. B.P. or A.D. 841 (Usami, 1996), the average recurrence interval is 515 to 840 years, and the elapsed time since the most recent event is 1159 years (Okumura et al., 1994). This result clearly demonstrates the high potential of

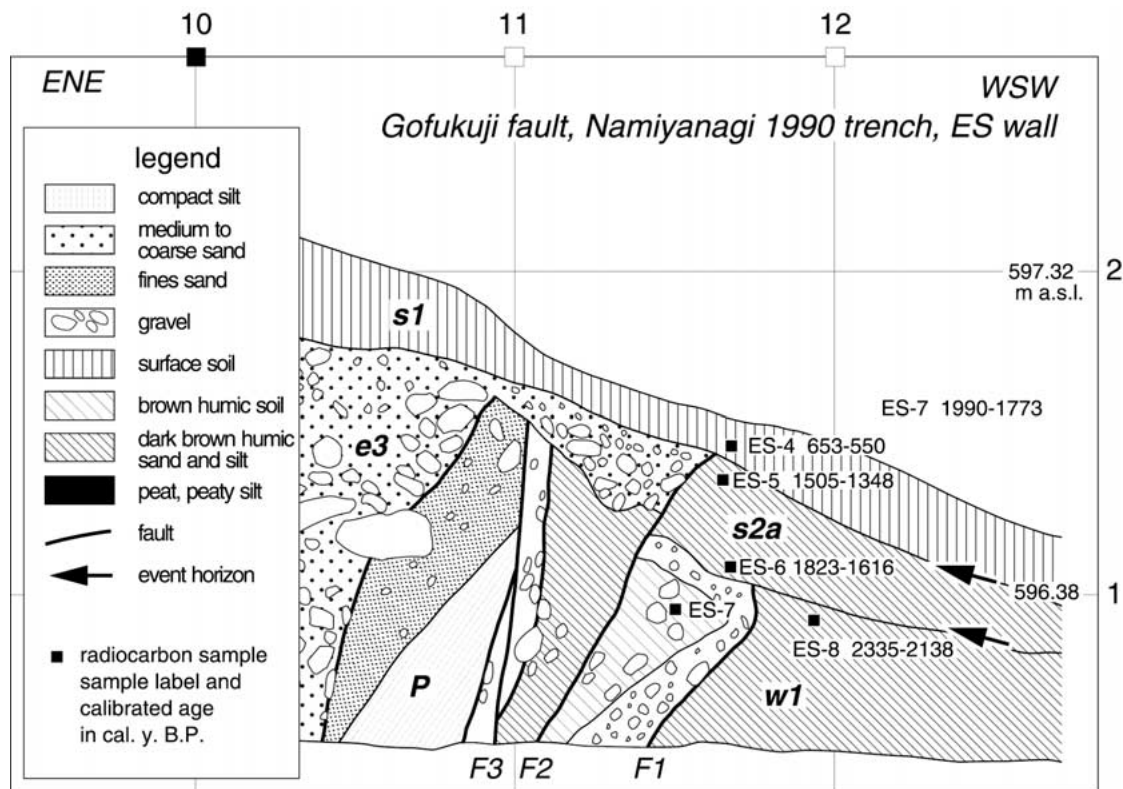


Figure 5. Map of the fault zone on the ES wall (modified from Okumura et al. 1994, Figure 8). The ordinate is actual length on slant wall of 50 to 60°.

a future earthquake on the Gofukuji fault because the elapsed time is hundreds of years longer than the average interval. However, the chronological constraints on these events are so poor that further studies were needed to obtain higher resolution of the timing of these paleoearthquakes. In addition, paleoseismological studies along all of the ISTL were needed to estimate the magnitude of future events based on the length of past ruptures.

#### Nakayama 1996 trenches

In order to confirm the high seismic potential from the Gofukuji fault with better chronological constraints, new paleoseismological studies were carried out at Nakayama in November 1996 shortly after the official warning regarding the risk of a large earthquake along the ISTL (Headquarters for Earthquake Research Promotion, 1996). The 1996 Nakayama trenches were located near the apparent southern termination of the Gofukuji fault (Figure 2A). Two trenches were excavated into the east slope of the Okubo-yama pressure ridge (Figure 6 inset). Trench A did not expose the

master fault zone, but it did expose an alternating sequence of slope deposits and buried A-horizons with minor shear planes, and recent sag-pond deposits. In trench B, a vertical fault plane juxtaposes a sequence of dark-colored buried soils (units s0 through s6) and colluvial deposits (w1 through w6) on east side against the conglomerate (P: 100 ka alluvial-fan deposits) that composes the pressure ridge (Figure 6).

The wedge-shaped colluvial deposits (units w1 through w6) probably indicate sudden exposure of the conglomerate on the slope by faulting and subsequent erosion and collapse of the conglomerate into a colluvial wedge. The present-day slope of the pressure ridge at the fault is less steep than the angle of repose, shows no evidence of failure, and is covered with dense vegetation. Based on the characteristics of the modern slope, it is not likely that any of the conglomerate would be exposed to generate slope colluvium without faulting. The modern A-horizon (unit s0) exposed in the trenches does not contain any conglomeratic colluvium other than a few scattering pebbles.

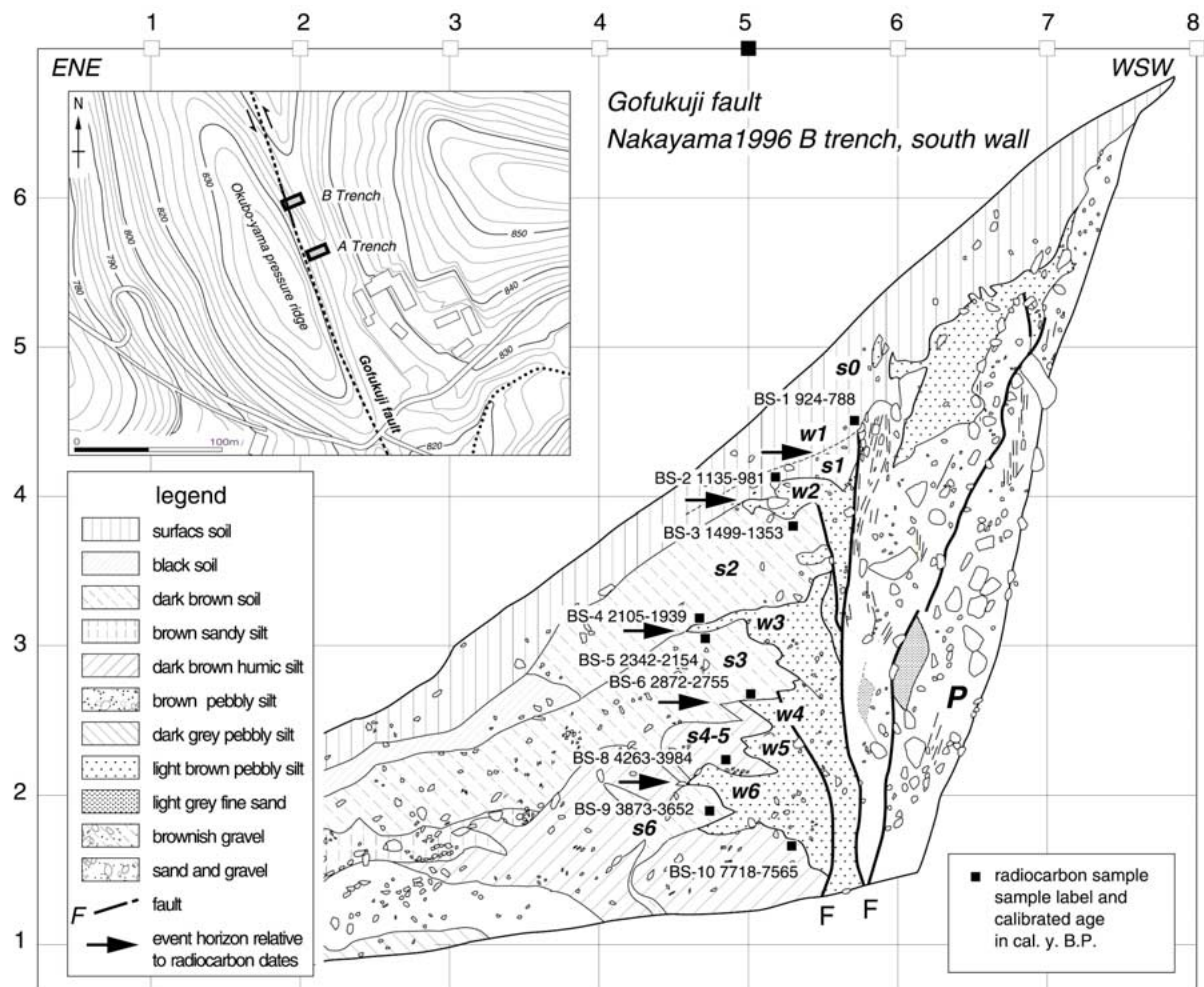


Figure 6. Map of the south wall of the Nakayama 1996 B trench. The ordinate is actual length on slant wall of 55°. Topographic map (inset) is based on Matsumoto City Office (1982).

The uppermost colluvial wedge (unit w1) is not as distinct as the other wedges below, but the truncation of the fault plane just below the BS-1 sample horizon is distinct, and unit w1 contains many more inorganic clasts than the overlying slope colluvium (unit s0). The last event occurred between the deposition of units s1 and s0. In the same manner, the penultimate and the antepenultimate events occurred between deposition of units s2 and s1, and between deposition of units s3 and s2, respectively. The wedge structures below unit s3 are not as clear because they are deformed by younger faulting events, but units w4, w5, and w6 probably indicate discrete old faulting events.

The radiocarbon dates shown in Figure 6 are derived mostly from bulk humic soil samples submitted for conventional  $\beta$ -counting methods. It is necessary

to carefully evaluate such bulk humic soil radiocarbon dates because these samples can be prone to reworking and contamination by younger organic carbon. However, in Nakayama B trench, the rate of soil accumulation is as high as 2 m in 4000 years and each buried A-horizon is separated by a colluvial wedge. This rapid deposition rate and the interlayered colluvial wedges probably minimized reworking and contamination of each buried soil layer. Hence the radiocarbon ages shown in Figure 6 are generally in correct stratigraphic order and are presumably reliable.

The ages of colluvial wedges are estimated as follows. Unit w1: 788 to 1135 Cal. y. B.P., unit w2: 981 to 1499 Cal. y. B.P., unit w3: 1939 to 2342 Cal. y. B.P., units w4, w5, and w6: 2755 to 4263 Cal. y. B.P. The ages of upper three wedges (units w1, w2, and w3) are

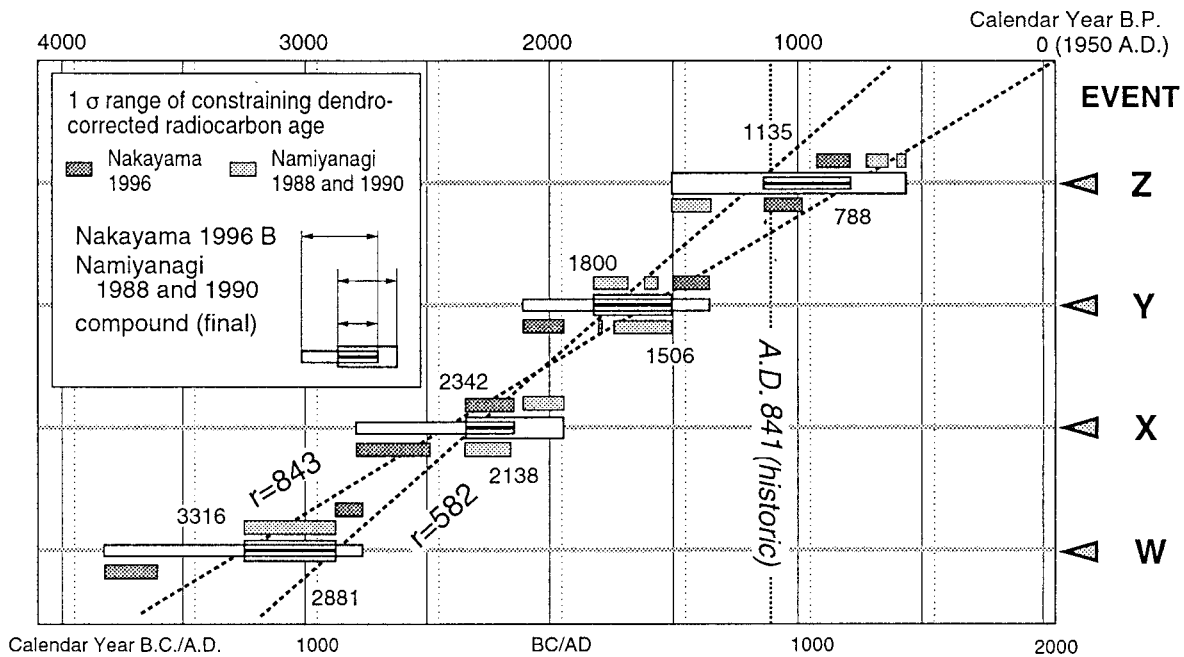


Figure 7. Diagram showing the age constraints of four prehistoric earthquakes on the Gofukuji fault. Event Z may correlate with a major historical earthquake that occurred in A.D. 841

interpreted as the ages of three earthquake events. The dates below and above unit w6 are inverted, and there is no age control between units w4 and w5. However, it is reasonable to assume that two or three events occurred before 2755 and after 4263 Cal. y. B.P., but it is not possible to separate the individual timing of these events.

The timing of at least 3 events at the Namiyanagi site coincides with the timing in the Nakayama B trench (Figure 7). The formation of colluvial wedges w1, w3, and w4 in the Nakayama B trench are correlatable with the events Z, X, and W at the Namiyanagi site. The age of w2 does not overlap that of the event Y in  $1\sigma$  range, however there is a possibility that the formation of w2 coincides with the event Y, which occurred around 1500 Cal. y. B.P. These results confirm the past time-series of earthquake events on the Gofukuji fault and refined the chronological constraints. Thus the revised estimates of the recurrence interval for four surface-faulting earthquakes on the Gofukuji fault without historic information is between 582 and 843 years. Assuming that the last event on the fault

occurred in 841 A.D. (Usami, 1996), it is between 680 and 825 years.

### Paleoseismology of the Northern ISTL

#### Outline of the Northern ISTL

The ISTL fault system north of Matsumoto (Northern ISTL) consists of east-dipping reverse faults on the east side of the Hida mountains. The fault system has created a narrow, N-S trending tectonic depression (Kamishiro basin, Figures 1 and 8A) and, east of the fault system, the Saikawa Hills, which formed in the Quaternary and are composed of Neogene sediments. In 1995 and 1996 Okumura et al. (1998b) excavated three exploratory trenches in the Northern ISTL to determine the rupture history on this part of the ISTL and to understand the possible interaction with the Gofukuji fault. This section summarizes the paleoseismological information from the Northern ISTL and discusses possible links among the Northern ISTL, the Gofukuji fault, and the Middle ISTL.

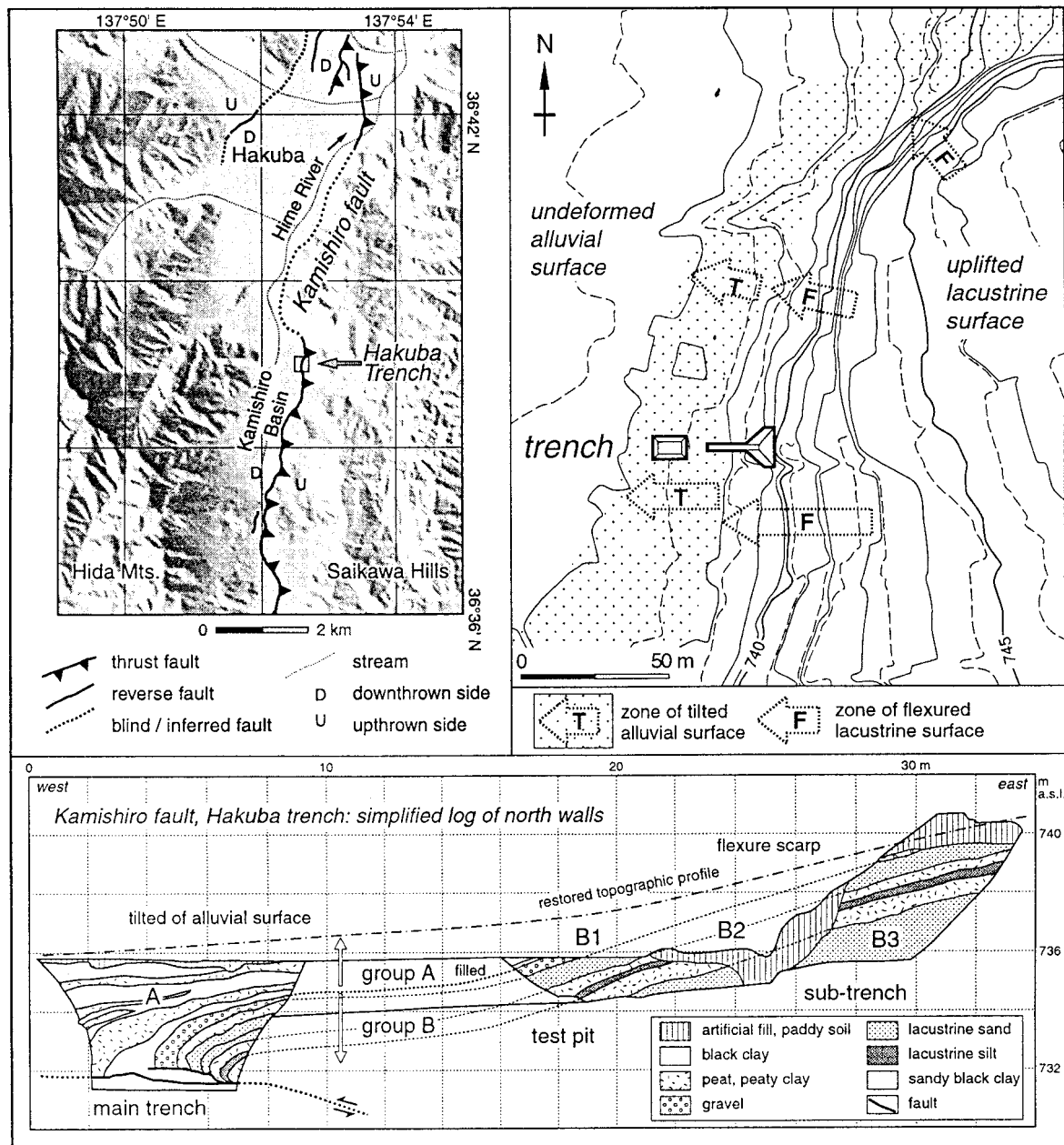


Figure 8. 8A (left): Topography along the Kamishiro fault based on 50 m DEM of Geographical Survey Institute (1997) mapped using GMT (Wessel and Smith, 1995). 8B (upper right): Detailed topographic map showing the Hakuba trench, flexure scarp of the Kamishiro fault, and tilted alluvial surface (modified from Okumura et al., 1998b, Figure 3). Detailed topographic map is unpublished data of the Topography Section, Geological Survey of Japan. 8C (lower right): Simplified geologic cross-section of the lacustrine sediments (B1, B2, and B3) and alluvial deposits (A) in the Hakuba trench (modified from Okumura et al., 1998b, Figure 4).

The northern ISTL contains two major strands: the Kamishiro fault on north and the East Matsumoto Basin fault (EMBF) on south. The estimates of vertical slip-rates range 1.5 to 3 m/ka during the past 20 to 30 ka (Shimokawa et al., 1995). Based on studies of shallow (20m) subsurface geologic structure at Hakuba trench site (Imaizumi et al., 1997) (Figure 8), the net slip is estimated to be 1.5 to 1.7 m/ka on a thrust fault of dipping 20° E. Unless we assume a very low-angle thrust, the net slip is probably about 2 to 3 m/ka, which is much less than that of the Gofukuji fault. If correct, this raises the problem of whether the Northern ISTL always ruptures together with the Gofukuji fault or whether it ruptures in a different time-series than the Gofukuji fault. This information is important to understand the magnitude and frequency of future earthquakes on these major fault systems. The first step to solve this problem is to understand the rupture history of the Northern ISTL.

#### *Hakuba trench on the Kamishiro fault*

The Kamishiro fault is located east of the Hime River along the foot of Saikawa Hills. The hills are composed of uplifted Miocene and Pliocene sediments (Figure 8). In the Kamishiro Basin, the fault trace is partly located within this late Quaternary sedimentary basin, about 100–300 m west of the base of the hills. The Hakuba trench was excavated across a fault scarp that separates a 10-ka lacustrine terrace surface on the east from the alluvial lowland in west. Aerial photographs and a detailed topographic map (Figure 2B) made before the surface was extensively graded in the 1970s show a zone of complex deformation along the fault. The trench shows that a convex flexure dipping about 20°W is associated with the scarp, and a 30- to 40-m-wide zone of the alluvial surface is tilted to the west along the foot of the scarp. The subtle tilt is only 2–3° to the west, but it is distinctive compared with the level marsh surface further to the west. This subtle topography is evidence that repeated faulting events have raised the lacustrine surface at the eastern end of the trench and that the most recent event has deformed the alluvial sediment on west side of the fault. The deformation is also clearly visible in trench walls (Figure 2C).

The sediments in the Hakuba trench are divided into the 8500 to 9900 Cal. y. B.P. lacustrine deposits (units B1, B2, and B3) and the 6700 to 800 Cal. y. B.P. alluvial deposits (units A1 through A7). The youngest alluvial deposits were removed to make the

paddy surface level. The lacustrine deposits that form the terrace surface are flexed down to the west and are cut by subhorizontal fault planes near the bottom of the main trench. The alluvial deposits, which were spread across the scarp and partly overlap on the flexure, consist of very loose, peaty silt, clay, and fresh peat full of twigs and grasses. These deposits were so soft and wet that it was impossible to extend the trench westward to examine the upper termination of the fault plane. The overall tectonic feature at this site is westward flexure in the hanging wall of a west-directed thrust fault. The asymmetry of the folded lacustrine layers is probably due to drag along the fault and plastic gravitational deformation of the tip of the hanging wall (Figures 8 and 9).

#### *Recognition of faulting events and their ages in Hakuba trench*

Since it was not possible to expose the upper termination of the fault, recognition of faulting events is mostly based on the deformation recorded in the alluvial sediments. Recognizing these events is based on the assumption that, as the peat and silt/clay in alluvial lowland accumulated, they formed a level surface. This assumption is reasonable because the surface of the modern alluvial lowland is very flat and covered with a peat layer. The black humic silt and clay layers of units A1, A3, A5, and A7 (Figure 8) consist of loose and massive sediments that are probably laid down in the still water of a marsh, and thus, formed level depositional surfaces. Unless tectonic deformation distorts the layers, the depositional surfaces should remain flat, and the stratigraphic layers should be of uniform thickness. Based on the deformation of the layers in the Hakuba trench, four faulting events were recognized. They are named H4, H3, H2, and H1 event in descending order.

Event H4 (most recent event): The tilted modern alluvial surface along the foot of fault scarp is evidence of the most recent faulting event at the Hakuba trench site. The gentle westward dip of units A1, A2, and A3 in the trench (Figure 9) is concordant with the gently sloping alluvial surface. The thickness of unit A2, and the total thickness of units A2 and A3 are uniform across the trench wall, which demonstrates that units A1, A2, and A3 have been deposited without any tectonic deformation. Therefore, the last event occurred after the deposition of unit A1. Three samples constrain the age of unit A1; N12 (grass fragments,  $\beta$ -counting), N13 (bulk organic clay,  $\beta$ -counting), N16

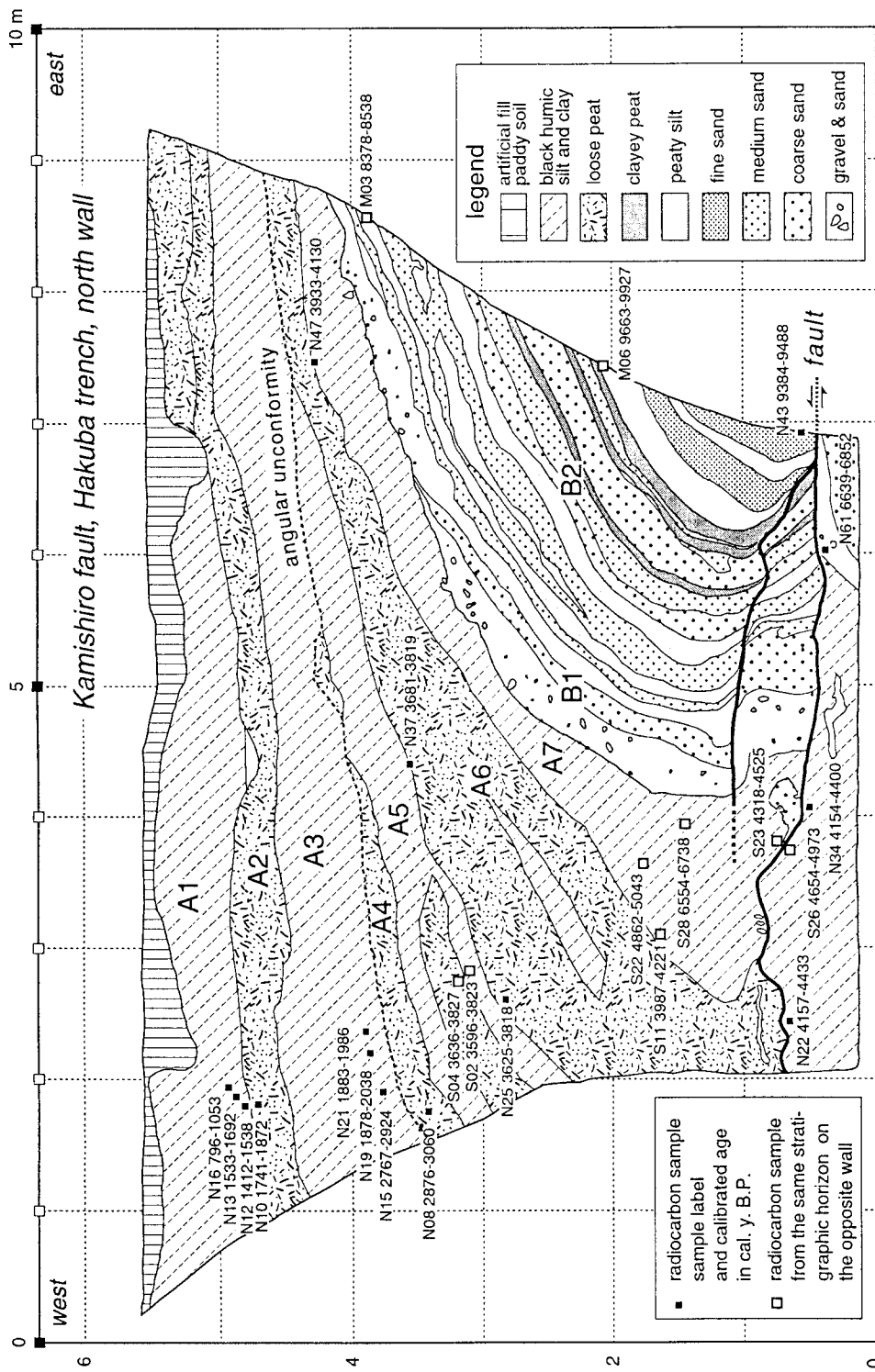


Figure 9. Map of the north wall of the Hakuba main trench (modified from Okumura et al., 1998, Figure 5). The ordinate is actual length on the slant wall of 55°.

(wood root,  $\beta$ -counting). Of these three, the date of sample N12 (1412 to 1538 Cal. y. B.P.) is preferred because sample N13 contained some reworked organic material and sample N16 might be a root that is much younger than the alluvial deposit. Based on our interpretation, the most recent event at this site occurred after 1412 to 1538 Cal. y. B.P.

Event H3 (penultimate event): A distinct angular unconformity is present below unit A3 as shown by layers below unit A3 dipping more steeply to the west than the strata above unit A3. The tilting of the older units and subsequent erosion are interpreted as evidence of the penultimate faulting event. The westward dip of angular unconformity between units A3 and A4 is roughly a half as steep as the westward dip of the boundary between units A5 and A6 in the middle part of the trench wall. This increased tilting is evidence of additional coseismic deformation of the older sediments. Event H3 occurred after deposition of unit A4 and before deposition of unit A3. Thus, the event postdates the age of sample N08 (wood in peat,  $\beta$ -counting: 2878 to 3060 Cal. y. B.P.) and predates the ages of samples N15, N19, and N21. The ages of samples N21 (grass fragment, AMS: 1883 to 1986 Cal. y. B.P.) and N19 (small twig, AMS: 1878–2038 Cal. y. B.P.) are preferred for the upper limit of the age of H3 event because sample N15 (bulk humic clay,  $\beta$ -counting: 2767 to 2924 Cal. y. B.P.) might contain reworked organic material from unit A4 and lower units. Thus, the preferred age for event H3 is between 3060 and 1878 Cal. y. B.P.

Event H2: Below the horizon of the H3 event, unit A6 thickens rapidly to the west in the bottom of the trench. This abrupt increase in thickness is unique in the trench and no other alluvial units above unit A6 have similar thickness changes. Since the upper contact of unit A7 was originally level before the deposition of unit A6, unit A7 must have been bent and deformed before or during deposition of unit A6 to allow for the increased thickness of unit A6. Faulting event H2 is interpreted as the cause of the deformation of unit A7 and the westward thickening of unit A6. Event H2 postdates the age of sample N47 (small twig, AMS: 3933–4130 Cal. y. B.P.) and predates the ages of samples N25 (small twig, AMS: 3625 to 3818 Cal. y. B.P.) and N37 (small twig, AMS: 3681 to 3819 Cal. y. B.P.). This faulting event is interpreted to have occurred between 4130 and 3625 Cal. y. B.P.

Event H1: Similar to unit A6, unit A7 also abruptly increases in thickness towards the fault. The thickness change of unit A7 is also reflected in the uneven con-

tact with unit B1; the irregularity in this contact is less than 0.5 m. Overall, unit A7 thickens by more than 1 m, which is much larger than the irregularity. Therefore, this thickening of unit A7 is interpreted as evidence of tectonic deformation. Based on this interpretation, at least one faulting event occurred during the deposition of unit A7. More than one event in unit A7 is likely because compaction of the unit should have reduced the apparent increase of the thickness toward the fault plane. The thickened horizon is between radiocarbon samples S22 (bulk humic silt,  $\beta$ -counting: 4862 to 5043 Cal. y. B.P.) and S28 (bulk humic silt,  $\beta$ -counting: 6654 to 6738 Cal. y. B.P.). Based on the age of these sample, the faulting event is interpreted to have occurred between 4862 and 6738 Cal. y. B.P.

These four faulting events occurred after 6738 Cal. y. B.P., and the most recent event postdates 1538 Cal. y. B.P. According to historical records, no large earthquakes have been reported after A.D. 841. in this area (Usami, 1996). Considering this historic information, the average recurrence interval for the four events ranges between 1108 and 1876 years. However, the average interval for the three recent events of 1258 to 1510 years (assuming the last event to be A.D. 841) is more reliable because event H1 may include more than one event. In conclusion, the Kamishiro fault has an average recurrence interval of 1258 to 1510 years in the middle and late Holocene, and the elapsed time since the last event is probably 1159 years but could be as much as 1538 years.

#### *Omachi trench on the East Matsumoto basin fault*

The East Matsumoto basin faults (hereafter referred to as EMBF) are a series of east-dipping reverse faults along the eastern margin of the Matsumoto basin (Figure 10A). The 10-km-long southernmost portion of the EMBF might be the northern extension of the Gofukuji fault (See section 2–2.). Here the geomorphic expression of this portion of the EMBF is not clear because of severe erosion, but Shimokawa et al. (1995) reported a significant amount of west-side-down dip-slip.

From Omachi northward, the EMBF runs along the foot of Saikawa Hills and displaces the alluvial fans and stream terraces similar to those near the Omachi trench site (Figure 10B). From Omachi southward, one strand of the EMBF runs along the base of the hills and another strand is located ~1 km west of the hills in the Matsumoto basin. The area between the two strands contains uplifted Late Pleistocene terraces,

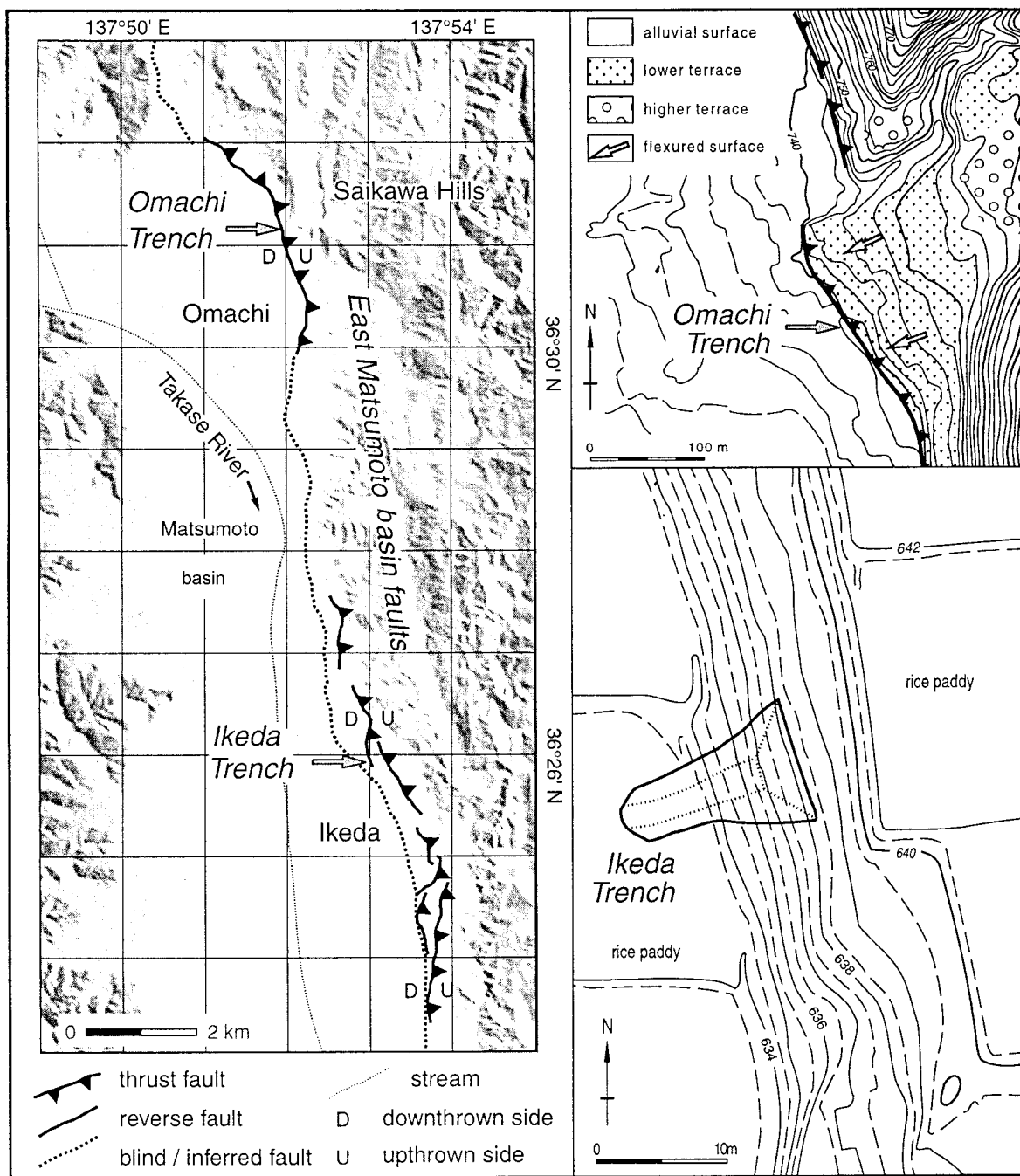


Figure 10. 10A (left): Topography along the East Matsumoto basin faults (EMBF) based on 50 m DEM of Geographical Survey Institute (1997) mapped using GMT (Wessel and Smith, 1995). 10B (upper right): Detailed topographic map around the Omachi trench (modified from Okumura et al., 1998b, Figure 7). Detailed topographic map is based on 1/2500 topographic map of Omachi city. 10C (lower right): Detailed topographic map around the Ikeda trench (modified from Okumura et al., 1998b, Figure 10).

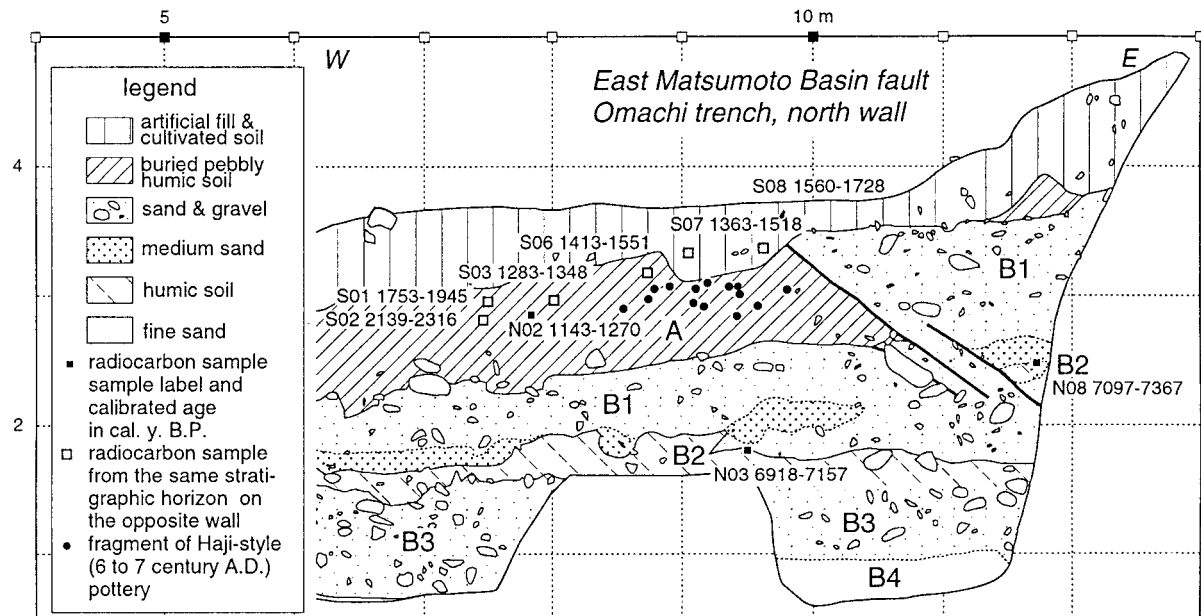


Figure 11. Map of the north wall of the Omachi trench (modified from Okumura et al, 1998b, Figure 8). The ordinate is actual length on the slant wall of 60°.

which are present only east of the inferred basin faults. Most of the western strands have been eroded by the Takase River, but the general location of these strands is defined by the distinctive topography and subsurface geology between the uplifted area to the east and subsiding area to the west (Figure 10A; Shimokawa et al., 1995).

East of Omachi City, a series of recent alluvial-fan surfaces have a cumulative offset of more than 10 m. A trench across a 1-m-high step at the foot of an about 10-m-high flexure scarp (Figures 10B and 11) exposed a reverse fault that displaces a gravel bed. This gravel bed (unit B3, Figure 11) has an age of about 7000 Cal. y. B.P. based on the radiocarbon age of a soil layer in the gravel. The fault also displaces a humic soil layer (unit A) that contains pottery fragments that are typical of the 6th to 7th century A.D. in this region (Figure 11; Personal Communication: Omachi City Board of Education). Since the pottery fragments are in the soil that is cut by and is under the fault, the last faulting event postdates 6th or 7th century A.D. The stratigraphic relations in this trench show that the faulting was not contemporaneous with the pottery but it occurred after a period of time during which the overlying soil accumulated.

In this trench, there are no constraints on the minimum age for the last event, but this information is provided by topographic and archaeological evidence from an alluvial fan 500 m south of the trench. The alluvial fan is composed of debris-flow deposits that are undeformed across the trace of EMBF. Archaeologists have found artifacts of the Heian Period (A.D. 781 to 1185: personal Communication: Omachi City Board of Education) on the surface of the debris flows, so these deposits coincide or predate the Heian Period. Therefore, the last faulting event in and around the Omachi trench occurred after 6th to 7th century A.D. and before 781 to 1185 A.D. The 8th to 10th century A.D. is the preferred time for the most recent event considering the pottery horizon in the trench and the historical records. The faulting in the trench likely correlates with the A.D. 841 earthquake (Usami, 1996).

#### *Ikeda trench on the East Matsumoto basin fault*

The Ikeda trench on EMBF is located on an uplifted terrace surface between the Saikawa Hills and the western strand of the EMBF (Figure 10A). At this location, the inferred fault trace east of the town of Ikeda bifurcates toward the north, and an east-

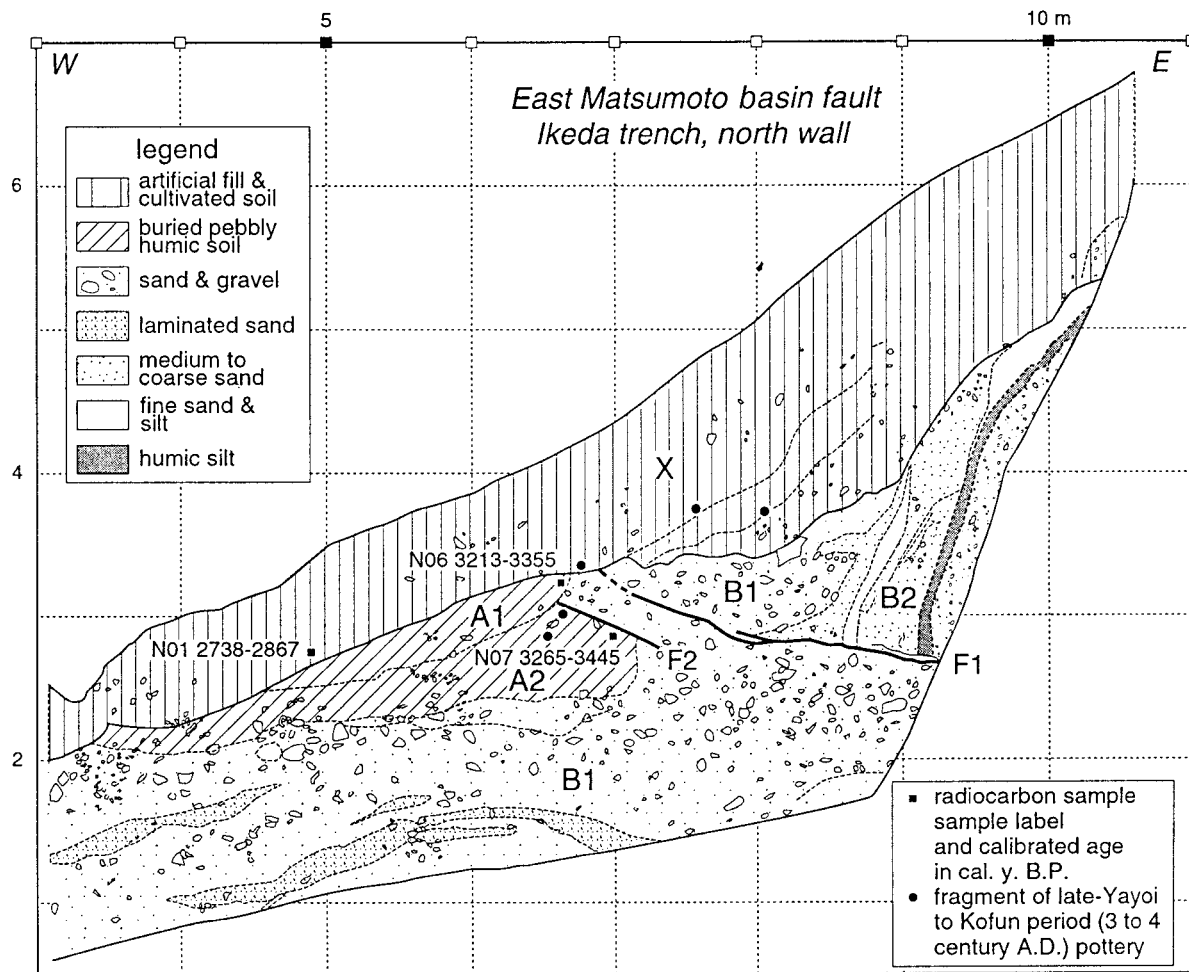


Figure 12. Map of the north wall of the Ikeda trench (modified from Okumura et al, 1998b, Figure 11). The ordinate is actual length on the slant wall of  $60^\circ$ .

ern strand deforms a terrace surface. Although the fault topography at this site is modified by rice fields, 6- to 7-m-high fault scarp is distinct on the terrace surface (Figure 10C). The Ikeda trench exposed similar geologic structures to those in the Hakuba trench (Figure 12). A low-angle thrust fault offsets terrace deposits of unit B1 and older deposits. Movement on the fault has thrust these older deposits over younger buried humic soil A-horizons (units A1 and A2). Although the upper part of the faulted deposits have been removed and covered with artificial soil (unit X), it is possible to estimate the maximum age limit of the faulting from the pottery fragments found in the undisturbed soil (unit A2) under the fault planes. The pottery fragments from unit A2 are of Late Yayoi to Kofun Period (3rd to 4th century A.D.: personal Com-

munication: Ikeda Town Board of Education). Three radiocarbon samples from this trench yielded anomalously old ages that suggest the samples have been contaminated by old carbon. Therefore, the age of the pottery fragments provides the only constraints on the timing of the event in the Ikeda trench.

#### *The recent activity of the Northern ISTL*

The results from Omachi and Ikeda trenches do not precisely constrain the timing and extent of the most recent faulting event on the EMBF. However, the fault trace of EMBF and surrounding geologic structures do not show any major geometric discontinuities that suggest the presence of a significant rupture segment boundary. Therefore, it is likely that the 33-km-long

EMBF has ruptured as a single segment during the last earthquake. This last event probably occurred in A.D. 841.

For the Kamishiro fault, the maximum age for the most recent event is estimated to be 1538 Cal. y. B.P. The minimum age for this event remains unknown. Although the age constraints on the most recent event are poor, it is possible that the most recent event was contemporaneous with the most recent event on the EMBF. This possibility is based on two observations. First, there is no other known contemporary historical earthquake in the region after the A.D. 841 event. Secondly, there is no geological evidence to indicate that a segment boundary exists between the Kamishiro fault and the EMBF. Both of these faults have comparable slip-rates, similar styles of deformation, and no significant gap or stepover is present between them.

The recurrence interval of 1258 to 1510 years for surface-faulting earthquakes on the Northern ISTL was estimated only from the Hakuba trench. This recurrence interval is significantly longer than that of the Gofukuji fault.

### **Hazard assessment of the Middle and Northern ISTL**

#### *Synthetic rupture history of the Middle and Northern ISTL*

The paleoseismological information from 11 trenches at nine locations (Figure 13) and the estimated slip rates (Figure 1 inset) along the Middle and Northern ISTL, permit the following conclusions:

- (a) The Gofukuji fault has the highest slip-rate (5–14 m/ka) and the shortest recurrence interval (582 to 843 years) of the faults studied. The slip during the last event was 6 to 9 m, which agrees with the slip per event estimate reported from the Chino trench (>6 m) (Research Group for Ito-Shizu Tectonic Line Active Faults, 1988).
- (b) The remainder of the Middle ISTL from Okaya southward to Kobuchizawa is characterized by a high rate of left-lateral slip (3–11 m/ka: Fujimori, 1991), but the previously reported recurrence interval of 3500–5000 years (Research Group for Ito-Shizu Tectonic Line Active Faults, 1988; Togo and Research Group for the Excavation of Okaya Fault, 1988; Okumura et al., 1998c) is much longer than that of the Gofukuji fault. The recurrence interval for the Middle ISTL appears to be too long relative to the high slip-rate.
- (c) The Northern ISTL has a rather uniform slip-rate of 2–3 m/ka, and an east-side-up vertical displacement. The Kamishiro fault in this part of the ISTL has an intermediate recurrence interval of 1258–1510 years.
- (d) The trenching studies and geomorphic evidence suggest that the entire Northern and Middle ISTL segments may have ruptured in A.D. 841 earthquake. Event Z on the Gofukuji fault, event H4 on the Kamishiro fault, and the most recent event on the EMBF all could be related to the A.D. 841 earthquake. Although the uncertainties for these events are large, the time of the last event is after the 5th century A.D. and before A.D. 841, assuming that no significant events are missing from the historical records. Geologic evidence from all of the study areas generally supports this possible scenario, as well as information on the time of the last event on Middle ISTL at Chino (Research Group for Ito-Shizu Tectonic Line Active Faults, 1988) and Kobuchizawa (Okumura et al., 1998c). Unfortunately, there is no evidence in the geological record or in historical accounts to show if the A.D. 841 earthquake was a single or multiple event. The 110-km-long section of faults might have ruptured by a single event in A.D. 841 or in A.D. 762 (Matsuda, 1998), or they might have ruptured in multiple events. Details of the rupture history of these faults remain unclear because the historical and geological records only indicate that the most recent ruptures on these faults occurred between 5th century A.D. and A.D. 841. More than one earthquake could have ruptured entire Middle and Northern ISTL in this period. Compared to recurrence intervals of several hundred to a few thousand years for these faults, the time period between the 5<sup>th</sup> century A.D. and A.D. 841 is short enough to be considered as a period of clustered earthquake activity in the ISTL.
- (e) Prior to the last event, the event Y on the Gofukuji fault was not contemporaneous with the penultimate event H3 on the Kamishiro fault. The timing of the event W on the Gofukuji fault does not coincide with either event H2 or event H3 on the Kamishiro fault; however, event X might possibly coincide with event H3. The correlation of events shown in Figure 13 demonstrates that the Gofukuji fault ruptures twice as frequently as the Kamishiro fault. Events Z and H4, as well as event X and H3, might have occurred at the same time, or at least within a time span of a few

hundred years. The paleoseismic evidence of prehistoric earthquakes on these faults suggests that the Northern ISTL ruptures together with the Gofukuji fault when the Northern ISTL is critically stressed and close to failure. Apparently, this occurs once on the Northern ISTL for every two major earthquakes on the Gofukuji fault.

#### *Modeling the future earthquake in the ISTL*

Judging from the recurrence interval, the probability of a major, surface-rupturing earthquake on the Gofukuji faults is high but the probability of a surface-rupturing earthquake on the rest of the Middle ISTL is considerably lower. The elapsed time of about 1200 years since the last event is equal to or exceeds the average recurrence interval of the Kamishiro fault in the Northern ISTL. The next surface-faulting event will probably rupture the Gofukuji fault, and it may trigger rupture on the Northern ISTL. Based on the geological record of prehistoric earthquakes, it is unusual for both faults to rupture in two successive events on the Northern ISTL. However, this unusual sequence might occur during the next surface-faulting event because of the unusually long quiescence time on the Gofukuji fault since the last event.

The long recurrence time from faults in the Middle ISTL south of Okaya compared to the rest of the Middle ISTL suggests that the Middle ISTL south of Okaya will not rupture during the next event on the Gofukuji fault. This conclusion is based solely on previous estimates of the recurrence intervals for the Middle ISTL (Okaya, Chino, and Kobuchizawa). However, alternative hypotheses on the future activity of the Middle ISTL have been proposed on the basis of estimated slip-rates and revised time series.

With considerable emphasis on the slip-rate information, Matsuda (1998) hypothesized that the next event on the ISTL might rupture the entire Northern and Middle sections and generate an earthquake of magnitude  $\sim 8$ . The Japanese Government's official warning (Headquarters for Earthquake Research Promotion, 1996) is based on this hypothesis, which is determined only from the empirical relationships between slip-per-event and rupture length, and between rupture length and magnitude. Matsuda (1998) used the high slip rate (9 m/ka: 11 m has accumulated since the last event) and the large slip-per-event (6–9 m) of the Gofukuji fault as a key to evaluate the likelihood of a future earthquake. Empirical relationships (Matsuda, 1975; Wells and Cop-

persmith, 1994) show that this amount of slip is usually associated with about 100 km of surface rupture and magnitude 8 earthquakes. A magnitude 8 earthquake would probably rupture the entire Northern and Middle ISTL.

Ongoing studies of the paleoearthquakes in the Suwa basin suggest that surface-rupturing earthquakes are much more frequent on the Middle ISTL in Suwa basin compared to other parts of the ISTL. Trenching studies in the Suwa basin have been of limited value because of intense human activity and unstable geologic conditions, but new data from studies of sediments at the bottom of the Suwa Lake are providing useful information. Saito et al. (1998), Okumura et al. (1998a, 2000) have tried to obtain high-resolution data on fault movements by studying the lake deposits in Suwa Lake, which is in a pull-apart basin bounded by normal faults (Figure 1). The interim results are shown in Figure 13 (Suwa Lake). Based on preliminary results, they recognized 7 faulting events that occurred between 8000 Cal. y. B.P. and 1000 Cal. y. B.P. from abrupt changes of the chemical and physical properties of lake-bottom sediments. These changes occur because of the sudden deepening of the lake due to normal faulting earthquakes after gradual shallowing. These studies show that the average recurrence interval for deepening of the lake is about 1100 years, but additional studies will further refine details for prehistoric events that deepen the land.

This 1100-year recurrence interval is much shorter than the 3500–5000-year interval that was previously estimated from onshore trenches (Figure 13), however, this shorter recurrence interval is consistent with the high slip-rate estimates of 5–11 m/ka. One explanation for the apparently low activity derived from trenching studies is that the trenches were located on a single fault strand whereas the entire fault system contains many strands that form a flower structure. If individual earthquakes only rupture single strands, then trench studies on a one strand may not provide complete evidence of faulting on the entire fault system.

If the rupture history in the Suwa pull-apart basin accurately represents the activity of the entire Middle ISTL, then a recurrence interval of 1100 years or less is comparable to that of the Gofukuji fault. If this is correct, then the basis that Matsuda (1998) used for hypothesizing future earthquakes using the slip-rate does not contradict with the data on recurrence intervals.

For the Southern ISTL, recent studies by Toda et al. (2000) reported a very low slip-rate ( $<0.5$  m/ka), a

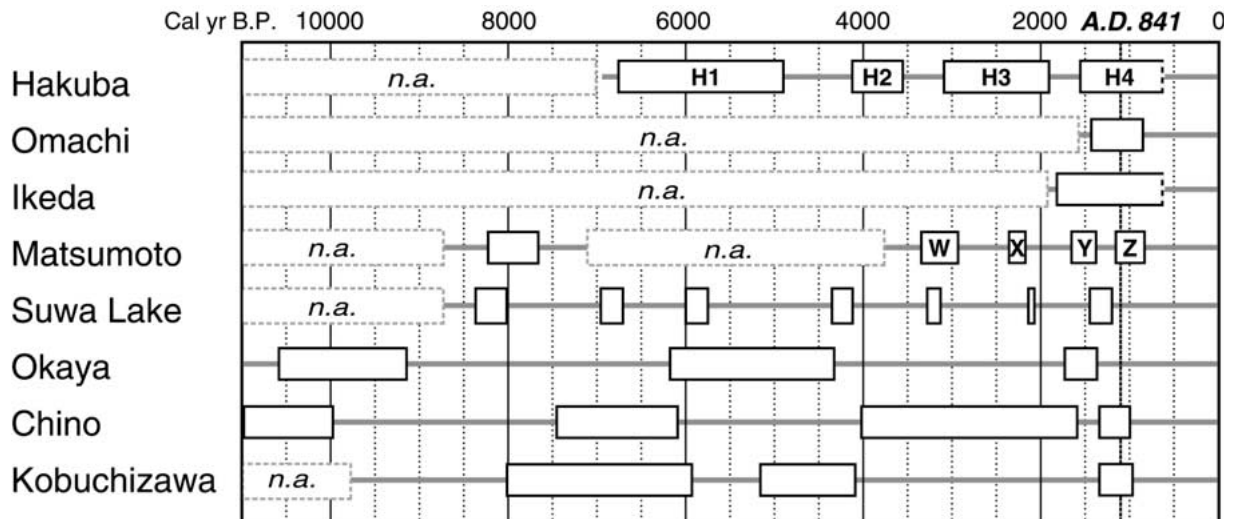


Figure 13. Timing of paleoearthquakes along the Middle and Northern ISTL. Each rectangular indicates the estimate age of individual event. Okaya: Togo et al. (1988), Chino: Research Group for the Ito-Shizu Tectonic Line Active Faults (1988), and Kobuchizawa: Okumura et al. (1998c). Suwa Lake: Preliminary results based on Saito et al. (1998) and Okumura et al. (1998a, 2000).

small slip-per-event (2 to 3 m), and a long recurrence intervals of more than 5000 years. Toda et al. (2000) concluded that the Southern ISTL did not rupture at the same time as the possible A.D. 841 event on the Middle ISTL. They also concluded that the probability of future synchronous rupture on the Southern ISTL with other parts of the ISTL is low. More detailed paleoseismological investigations are under way along the Southern ISTL, but based on Toda et al.'s conclusion, the Southern ISTL appears to rupture independently from other parts of the ISTL and is not discussed further in this report.

Three possible models can be considered for future surface-faulting earthquakes on the ISTL. These models do not exclude the possibility that ruptures can occur in multiple earthquakes, a possibility that cannot be discussed further here. The three simplified models are: (1) the Gofukuji fault ruptures by itself, (2) the Gofukuji fault and the entire Northern ISTL rupture together, and (3) the entire Middle and Northern ISTL rupture together. In the first case, the earthquake ruptures only the 20- to 30-km-long Gofukuji and adjacent faults, which would generate an event of about magnitude  $\sim 7.0$ . In the second case, the Gofukuji fault and the Northern ISTL rupture together, producing about 80 km of surface faulting and an earthquake of magnitude  $> 7.5$ . In the third case, the surface ruptures would be about 110 km long, and the associated earthquake would have a magnitude of about 8 (Matsuda, 1975, 1998; Wells and Coppersmith, 1994). The

paleoseismological data presented in this paper favor the second model, but additional high-resolution data from the Middle ISTL may eventually favor the third model.

Kumamoto (1998) estimated the conditional probability of earthquakes on active faults in Japan and suggested that the probability of an earthquake on the Gofukuji fault alone was 35 to 40% in next 100 years. This is the highest probability for any onshore active fault in Japan. Recent studies have confirmed the scientific basis for the Japanese Government issuing an official warning of high seismic risk on the ISTL (Headquarters for Earthquake Research Promotion, 1996). These studies have also provided better data that can be used to model the future earthquake probabilities. However, much more precise information on the past earthquakes is indispensable to reasonably prepare for the hazard.

#### Acknowledgements

The author wish to thank the landowners of the trench sites, local governments and archaeologists, colleagues in Geological Survey of Japan, universities, and consulting companies for their kind supports during the successful trenching studies. Warm encouragement of the editors and helpful comments by the reviewers very much improved the manuscript.

## References

- Allen, R.C., 1975, Geological criteria for evaluating seismicity, *Geol. Soc. Amer. Bull.* **86**, 1041–1057.
- Fujimori, T., 1991, Active faults in the Suwa basin, and its evolution as a pull-apart basin on the Itoigawa-Shizuoka tectonic line, *Central Japan. Geogr. Rev. Japan* **64A**, 665–696.
- Geographical Survey Institute, 1997, Digital map 1 km grid (Elevation), Geographical Survey Institute, Tsukuba, Japan, a Compact Disc.
- Geographical Survey Institute, 1997, Digital map 50 m grid (Elevation) Nippon-II, Geographical Survey Institute, Tsukuba, Japan, a Compact Disc.
- Headquarters for Earthquake Research Promotion, 1996, Report on the evaluation and survey results for Itoigawa-Shizuoka tectonic line active fault system (September 11, 1996), Headquarters for Earthquake Research Promotion, Prime Minister's Office [Currently available from: <http://www.jishin.go.jp/main/welcome-e.htm> (in Japanese)].
- Imaizumi, T., Haraguchi, T., Nakata, T., Okumura, K., Togo, M., Ikeda, Y., Sato, H., Shimazaki, K., Miyauchi, T., Yanagi, H. and Ishimaru K., 1997, Slip rates on the Kamishiro active fault along the northern part of the Itoigawa-Shizuoka tectonic line, detected by long geo-slicer and drilling, *Active Fault Res.* **16**, 35–43.
- Ikeda, Y. and Yonekura, N., 1986, Determination of late Quaternary rates of net slip on two major fault zones in central Japan, *Bull. Dept. Geogr. Univ. Tokyo* **18**, 49–63.
- Kumamoto, T., 1998, Long-term conditional seismic hazard of Quaternary active faults in Japan, *J. Seismol. Soc. Japan (Zisin)*, 2nd Series, **50**, 53–71.
- Matsuda, T., 1974, Surface faults associated with Nobi (Mino-Owari) earthquake of 1891, Japan, *Spec. Bull. Earthq. Res. Inst., Univ. Tokyo* **13**, 85–126.
- Matsuda, T., 1975, Magnitude and recurrence interval of earthquakes from a fault, *J. Seismol. Soc. Japan (Zisin)*, 2nd Series **28**, 269–282.
- Matsuda, T., 1998, Present state of long-term prediction of earthquakes based on active fault data in Japan, *J. Seismol. Soc. Japan (Zisin)*, 2nd Series **50**, 23–33.
- Matsumoto City Office, 1982, 1/2500 Topographic map, VIII-JC 38-4, Matsumoto City Office, Matsumoto, Japan, 1 sheet.
- Niklaus, T.R., 1991, CalibETH version 1.5b, ETH, Zürich, 2 diskettes and 151 pp.
- Okumura, K., Saito, K., Fukuzawa, H., Mizuno, K., Kariya, Y. and Fujiwara, O., 2000, Re-examination of the rupture history of the Itoigawa-Shizuoka tectonic line active fault system, *Chikyu Monthly*, Special issue **28**, 92–100.
- Okumura, K., and Tsukuda, E., 1995, 1988 Trenching study of the Gofukuji fault of the Itoigawa-Shizuoka tectonic line active fault system at Namiyanagi, Matsumoto, Central Japan, *Active Fault Res.* **13**, 54–59.
- Okumura, K., Shimokawa, K., Yamazaki H. and Tsukuda E., 1994, Recent surface faulting events along the middle section of the Itoigawa-Shizuoka tectonic line – Trenching Survey of the Gofukuji Fault near Matsumoto, Central Japan, *J. Seismol. Soc. Japan (Zisin)*, 2nd Series **46**, 425–438.
- Okumura, K., Fukuzawa, H., Saito, K., Mizuno, K. and Fujiwara O., 1998a, High-resolution Multi-proxy Analyses and Dating of Lake Deposits Affected by Recent Faulting Events: a Case Study of the Suwa Lake on the Itoigawa-Shizuoka Tectonic Line (ISTL), Central Japan, *EOS, Transactions, American Geophysical Union* **79**, F614.
- Okumura, K., Imura, R., Imaizumi, T., Togo, M., Sawa, H., Mizuno, K., Kariya, Y. and Saito E., 1998b, Recent surface faulting events along the northern part of the Itoigawa-Shizuoka tectonic line – Trenching survey of the Kamishiro fault and East Matsumoto basin faults, Central Japan –, *J. Seismol. Soc. Japan (Zisin)*, 2nd Series **50**, 35–51.
- Okumura, K., Mizuno, K., Fukuzawa, H., Saito, K. and Fujiwara, O., 1998c, *Paleoseismology of the middle part of Itoigawa-Shizuoka tectonic line active fault system*, Abstracts, 1998 Japan Earth and Planetary Science Joint Meeting, Tokyo, Japan, 26–29 May 1998, 317.
- Research Group for Active Faults in Japan, 1991, *Active Faults in Japan*, revised edition. University of Tokyo Press, Tokyo, 437 pp.
- Research Group for Ito-Shizu Tectonic Line Active Faults, 1988, Late Quaternary activities in the central part of Itoishizu tectonic line – excavation study at Wakamiya and Osawa faults, Nagano prefecture, central Japan, *Bull. Earthq. Res. Inst., Univ. Tokyo* **63**, 349–408.
- Saito, K., Fukuzawa, H., Okumura, K., Mizuno, K. and Fujiwara, O., 1998, *Anomalous layers in lake sediments from Lake Suwa and slip on the faults at the Suwa basin since 16,500 Cal. y. B.P.* Abstracts, 1998 Japan Earth and Planetary Science Joint Meeting, Tokyo, Japan, 26–29 May 1998, 197.
- Sato, H., 1996, Inversion tectonics of Japanese Islands, *Active Fault Res.* **15**, 128–132.
- Seno, T. and Sakurai, T., 1996, Can the Okhotsk plate be discriminated from the North American plate? *J. Geophys. Res.* **101**, 11305–11315.
- Shimokawa, K., Mizuno, K., Imura, R., Okumura, K., Sugiyama, Y. and Yamazaki, H., 1995, Strip map of the Itoigawa-Shizuoka tectonic line active fault system, *Tectonic Map Series 11*, Geological Survey of Japan, Tsukuba, Japan.
- Toda, S., Miura, D., Miyakoshi, K. and Inoue, D., 2000, Recent surface faulting events along the southern part of the Itoigawa-Shizuoka tectonic line, *J. Seismol. Soc. Japan (Zisin)*, 2nd Series **52**, 445–468.
- Togo, M. and Research Group for the Excavation of Okaya Fault, 1988, Rupture history of Okaya fault in the Itoigawa-Shizuoka tectonic line active fault system. Programme and Abstracts, *Seismol. Soc. Japan*, 1988 **1**, 6–8 April, 1988, Tokyo, 223.
- Usami, T., 1996, *Materials for Comprehensive List of Destructive Earthquakes in Japan* [revised and enlarged edition], University of Tokyo Press, Tokyo, 493 pp.
- Utsu, T., 1996, *A Catalog of Damage Earthquakes in the World*, an online WWW catalogue at the Earthquake Research Institute, University of Tokyo [<http://www.eri.u-tokyo.ac.jp/UTSU/index.html>].
- Wei, D. and Seno, T., 1998, Determination of the Amurian plate motion in mantle dynamics and plate interactions in East Asia, In: M. Flower et al. (eds), *Geodynamics Series 27*, American Geophysical Union, Washington, pp. 337–346.
- Wells, D.L. and Coppersmith, K.J., 1994, New empirical relationships among magnitude, rupture length, rupture width, rupture area, and surface displacement, *Bull. Seism. Soc. Amer.* **84**, 974–1002.
- Wessel, P. and Smith, W.H.F., 1995, New version of the Generic Mapping Tools released, *EOS Trans. Amer. Geophys. Union* **76**, 329.
- Working Group for Compilation of 1:2,000,000 Active Fault Map of Japan, 2000, New 1:2,000,000 Active Fault Map of Japan. An attachment map to Active Fault Research, 19.
- Yamazaki, H., Shimokawa, K., Mizuno, K. and Kashima, K., 1990, Subsurface geology and active faults in Suwa tectonic basin, Programme and Abstracts, *Japan Assoc. Quaternary Res.* **20**, 80–81.

